



Waviness analysis of glossy surfaces based on deformation of a light source reflection

Jiří Filip , Radomír Vávra, Frank J. Maile

Received: 1 June 2022 / Revised: 20 February 2023 / Accepted: 26 February 2023
© The Author(s) 2023

Abstract The evaluation of waviness, also known as orange peel, is essential for the quality control of materials in industrial fields working with high gloss materials, e.g., coatings, automotive and metal fabrication. This paper presents an affordable noncontact method for waviness analysis based on a single image of the light source reflected from the surface under study. The spatial perturbations along the contour of the light source reflection are compared to the ideal contour and analyzed in the Fourier domain to obtain standard features that have been compared to commercial ripple characterization device. Additional three method-specific features are proposed and evaluated. Our method has been tested on a set of ten orange peel standards, ten effect, and three solid coating samples and shows promising performance in waviness characterization of glossy surfaces.

Keywords Waviness, Orange peel, Measurement, Gloss, Highlight, Profile, Contour, Reflection

Introduction

In the coating industry, a variety of processes are used to finish coated surfaces. Many parameters such as the coating composition, application method, speed, and direction of movement of the application equipment, and the coating and drying temperature affect film formation (coalescence) and hence the final height

profile of the coating layer on the coated surface. This often results in an imperfect, nonplanar surface with standard deviations that become visible when the surface is viewed under locally directed surface illumination. An example is shown in Fig. 1a, in which the light reflection from an ideally flat surface is compared to a surface that has an additional ripple effect that causes the edges of the reflected light source boundaries to blur and/or shift.

These effects depend on the scale and can be divided into two categories. On a fine scale close to the resolution of the human eye (wavelengths shorter than 0.1 mm), we can distinguish the clarity of the reflected boundary and perform a physical measurement of the relationship between the intensity of the reflected light in the specular reflection and that of its near surroundings. Standard measures of such light scattering properties are referred to as dullness, DOI, or opacity. The industry uses generally accepted standard test methods for specular gloss,¹ DOI², and haze.³

Hunter et al.⁴ defined several categories of surface gloss and pointed out that a spatial displacement of reflected highlight is related to macroscopic smoothness of the reflected surface. Thus, at coarser scales, we can evaluate the displacement of specular light contours due to gradual changes in surface normals, resulting in specific texture structures visible in the reflected images. The term surface roughness is often used to describe wavelengths shorter than 0.8 mm, which corresponds to surface properties associated with local microgeometry. The structures above these wavelengths are generally referred to as waviness or orange peel, defined in the literature⁵ as the appearance of irregularity of a surface resembling the skin of an orange. For the purposes of this article, we will refer to them by the general term *waviness*, regardless of wavelength. Although the visual impact of orange peel is mentioned in the literature,² there is no recognized standard method for waviness assessment; however,

J. Filip (✉), R. Vávra
The Czech Academy of Sciences, Institute of Information
Theory and Automation, Praha, Czech Republic
e-mail: filipj@utia.cas.cz

F. J. Maile
Schlenk Metallic Pigments GmbH, Roth-Barnsdorf,
Germany

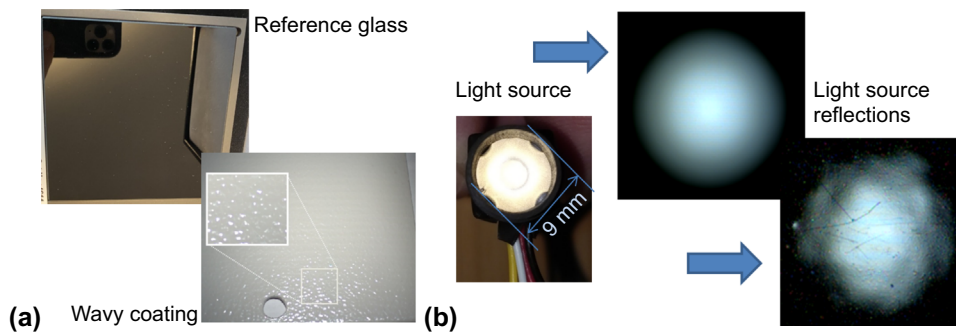


Fig. 1: An example of (a) two materials with different waviness and (b) the light source shape and its reflection

several commercial instruments exist that perform such analysis based on their own algorithms, e.g., wave-scan from BYK-Gardner⁶ and Rhopoint TAMS from Konica Minolta.⁷ The first instrument is based on frequency analysis of the reflection of a linear light source from a large area of the tested surface. This analysis provides accurate information about the surface profile, but requires a large sample size and an expensive instrument. The second instrument is based on deflectometry with phase measurement, which provides three-dimensional shape information of the surface profile and allows its further statistical analysis.

In contrast, we propose a nearly hardware-independent and affordable method for evaluating waviness based on the analysis of a single image of a circular light source reflection at a specular angle. On a set of 13 solid, 10 effect coating samples, and one glass reflectance standard, we evaluated the performance of our method and compared it with (1) orange peel standards, and (2) readings of the wave-scan device.⁶

This paper is organized as follows: “[Related work](#)” section discusses related work. “[Proposed method of waviness analysis](#)” section describes the principle of the proposed method. “[Experiments](#)” section presents our test samples, measurement setup and describes the results of our method, and compares it with orange peel standards and a commercial device. “[Discussion and limitations](#)” section discusses advantages and limitations of our method.

Related work

One of the first reviews on the application of angle-dependent optical effects resulting from submicrometer structures of films and pigments was published in.⁸ A detailed review of special effect pigments can be found elsewhere.^{9,10}

Unfortunately, there is limited research on analyzing the waviness or orange peel of coated surfaces. Brodman¹¹ analyzed the roughness and waviness of materials by deflecting light, resulting in a scattered light distribution with variable shape depending on the profile of the illuminated surface.

Konieczny and Meyer¹² proposed a rendering system for visualization of surface displacement due to orange peel effect obtained by means of BYK wave-scan measurements. Authors provide a system predicting appearance for different combinations of orange peel and surface gloss, performed its subjective evaluation, and concluded that orange peel visibility is color shade related. Sone and Watanabe¹³ proposed a method using spectral camera and telecentric lighting projecting a line pattern. They proposed an orange peel measure based on the frequency analysis of line deformation in the captured image and evaluated its performance in a psychophysical experiment. Leloup et al.¹⁴ proposed a novel image-based instrument for gloss measurement. The authors analyzed the effect of coating waviness on the Fourier spectrum of the gloss image and found that three ranges of the spectrum (low-pass, band-pass, high-pass) describe the presence of waviness at different magnitudes. They concluded that the exact limits of these ranges must be defined.

Similarly to the mentioned approaches, our method provides noncontact waviness analysis in the frequency domain, but also proposes additional method-specific computational features. In contrast to a related study¹³, our method does not rely on any specialized equipment, while still providing reliable results comparable to readings of a commercial device.

Proposed method of waviness analysis

Our method analyzes the deformation of the known shape of a circular light source in the image of its reflection at a specular angle. It evaluates the differences between the boundary of specular light and an ideal elliptical shape. Figure 1a shows two different samples, a smooth mirror and a rippled coating. When illuminated by a point light with a circular reflector, different images are obtained depending on the reflected surface. While a clear circular image is obtained for the glass mirror, the contour of the specular light is distorted for the rippled coating due to

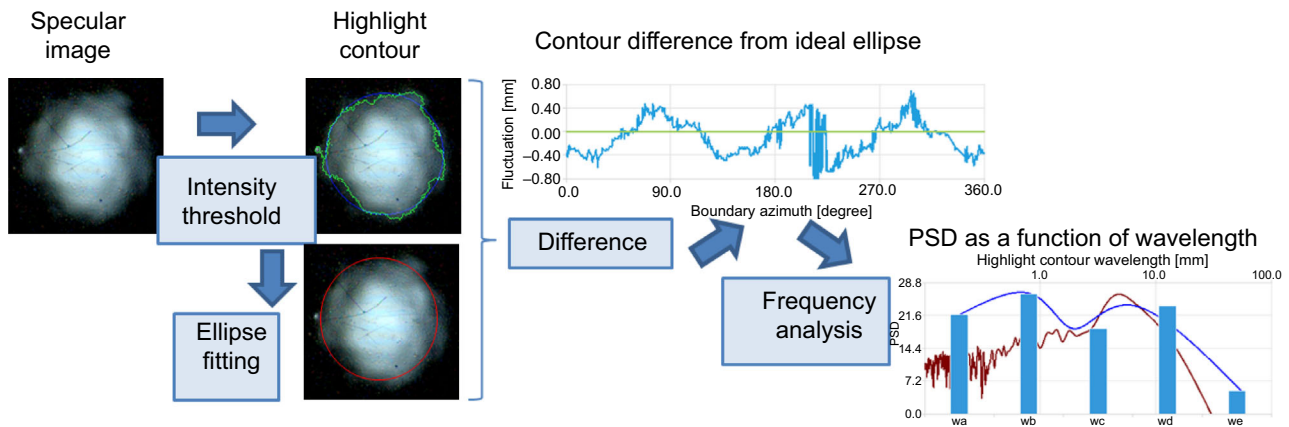


Fig. 2: A principle of the proposed waviness analysis method

local deviations of the surface normal from the material sample's normal, as shown in Fig. 1b.

The entire waviness analysis method is explained in Fig. 2. First, a custom threshold is applied to the image to preserve the outline of the highlights. This threshold only influences the area covered by the reflected ellipse and possibly has an effect on the captured range of wavelengths. In our experiment, we used threshold 30% of maximum highlight intensity to have a sufficiently large area of the reflected highlight while keeping the entire reflected boundary within the captured area. In the next step, we fit an ellipse to this contour to determine the center of the specular highlight and its size. Then, we use the ideal ellipse obtained for the reference glass mirror (shown in red) and change only its position and size by the estimated parameters of the tested sample. The ideal ellipse is obtained using the same procedure as described above.

Once we have contours of ideal flat reference and of the tested materials, we can calculate their difference. Since we know the pixel size from the camera resolution, we can obtain one-dimensional profile of surface deviations in millimeters by unfolding a circular difference between specular highlight boundary from the ideal ellipse as shown in Fig. 2.

We tested different specular angles and found that lower polar angles are more suitable for analysis due to the lower highlight intensity and better luminance uniformity due to a smaller span of the illumination and viewing angles along the surface contour. Additionally, according to gloss measurement standards¹ a specular geometry 20° is recommended for materials having gloss values over 70 GU. Therefore, we used the specular angle 15° .

Once we have the surface profile, we perform a Fourier transform and calculate the frequency spectrum. To obtain the energy of each frequency component, a power spectral density (PSD) of the spectrum is calculated, which is finally plotted as a function of the wavelength of the surface frequency in mm (red outline in Fig. 2). Following the procedure of the wave-scan device,⁶ the PSD is divided into five bins:

W_a : 0.1–0.3 mm, W_b : 0.3–1.0 mm, W_c : 1–3 mm, W_d : 3–10 mm, and W_e : 10–30 mm (blue outline and bars in Fig. 2). We also compute SW (short wavelength), LW (long wavelength) bins corresponding to ranges 0.3–1.2 mm and 1.2–12 mm, and their average AW.

Furthermore, we calculated three additional boundary-related features: (1) CA—a maximum amplitude of the contour profile difference from ideal ellipse (in mm), (2) CL—a circumference of the ellipse fitted to the highlight contour in mm (computed analytically from the ellipse parameters a and b), and (3) MA—a cumulative moving average difference from contour profile with neighborhood size 20 pixels.

Experiments

This section introduces our test datasets, describes the measurement setup, and shows the performance of our method.

Tested material samples

For the purpose of our analysis, two datasets were used.

First, we analyzed a set of ten ACT orange peel standards,¹⁵ black solid coatings with known instrumental orange peel magnitude ratings R obtained using BYK wave-scan device.

Second, we collected a set of glass standard shown in Fig. 1 (denoted as sample 0) and 10 effect coatings [six contain diffractive pigments applied using powder coating system (Nos. 1–6),¹⁶ four contain aluminum pigments (Nos. 7–10)]. A detailed list of the tested samples is given in Table 3. Figure 3 gives an overview of the surface variations of each sample. In the first row are photos of the coating plates taken with a point light source, and in the second row are the images of the specular highlights. The third row shows a texture of the specular highlight after a compensation of the

Table 3: A list of the tested effect coating samples

Nos.	ID	Pigment	Method	Basecoat	Details
00	REF	–	–	–	Black-coated glass reference
01	DPW1	Diffractive	Powder	White	Multiflect 150 μm
02	DPB1	Diffractive	Powder	Black	Multiflect 150 μm
03	DPW2	Diffractive	Powder	White	Multiflect 35 μm
04	DPB2	Diffractive	Powder	Black	Multiflect 35 μm
05	DPW3	Diffractive	Powder	White	Multiflect 20 μm
06	DPB3	Diffractive	Powder	White	Multiflect 20 μm
07	A1	Aluminum			AluMotion S08/CAB58 8 μm
08	A2	Aluminum			AluMotion S22/CAB58 22 μm
09	A3	Aluminum			AluMotion S22/CAB57 22 μm blue
10	A4	Aluminum			AluMotion S08/CAB57 8 μm blue

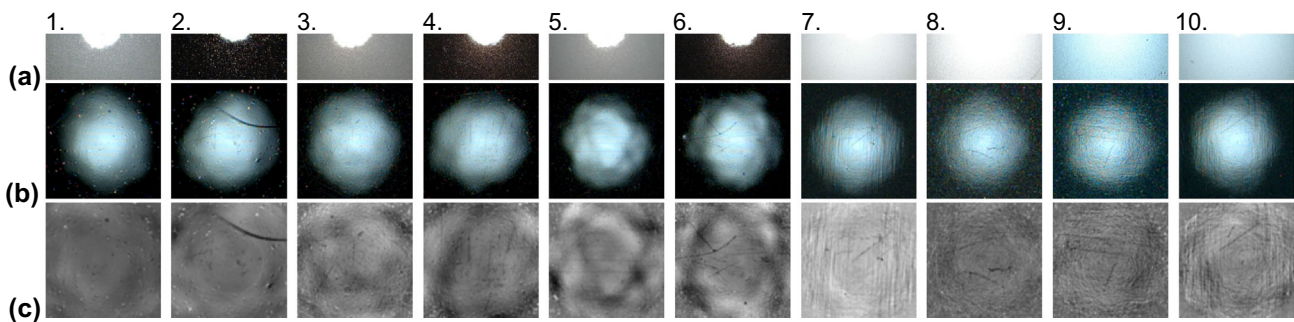


Fig. 3: Photographs of (a) sample, (b) of the specular highlight, and (c) its texture after a compensation of decreasing illumination intensity

illumination intensity, which decreases from the image center.

Third, the method’s performance was also demonstrated on three solid coating samples with challenging surface variations.

Measurement setup

A light source was used LED Cree XPG2 with cylinder-shaped reflector of diameter 10 mm and length 9 mm, as shown in Fig. 2. Images of light source reflections were captured by IDS CMOS camera UI-3591LE with sensor 1/2.3” of resolution 4912 x 3684 pixels (pixel size is 12.7 μm). The camera used an S-mount lens of f=25 mm. The light source was positioned approximately 250 mm and the sensor 320 mm from the scanned sample. The captured surface area was 15 × 15 mm², and image resolution was 2010 DPI. The camera was radiometrically calibrated and the high-dynamic range image of sample specular reflection was obtained by combining multiple light intensities and exposure times.

To avoid bias caused by capturing a nontypical area of the material sample, three photographs of a specular highlight were taken at different spatial locations. Each of them was processed independently, and the

obtained features of our methods were averaged. We also analyzed uniformity of maximum luminance across all three readings and its mean relative standard deviation within each triplet was 0.71%.

All image processing was performed on only one CIE luminance channel. Our method was implemented in OpenCV in C++ and MATLAB.

Results for orange peel standards

The estimated contours of specular highlights, their unfolded highlight contours profiles, and frequency analysis for ten ACT samples are shown in Fig. 4. We observe decreasing amplitude and gradually changing frequency content with increasing sample number. This behavior is reflected in different values of individual frequency bins shown as blue bars.

For ten ACT samples readings for individual bins $W_a \dots W_b$ and SW, LW, and AW features are obtained as well as readings of the proposed statistical features CA, CL, and MA. For each feature, three readings are averaged to avoid bias due to local sample nonuniformity. Standard deviations relative to mean values in % shown in the first row of Table 1 demonstrate that standard deviations are within 10% range with best uniformity for CA and MA features. We experimen-

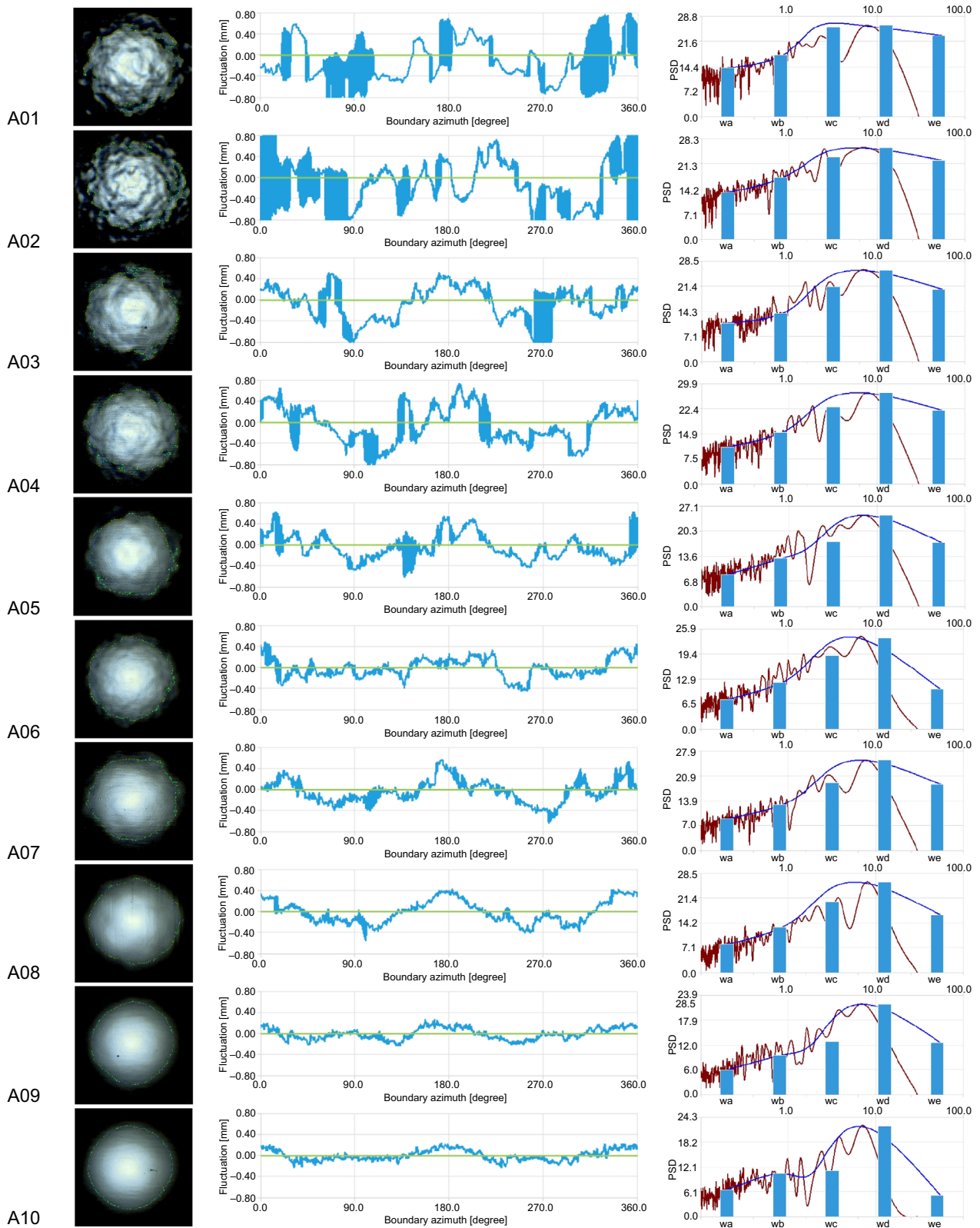


Fig. 4: ACT standard samples' highlight shapes at specular direction 15° with the estimated boundary, their unfolded boundary profile estimated as difference from the ideal ellipse, and PSD obtained by frequency analysis

tally verified that including additional readings does not significantly improve the deviation values.

In order to demonstrate a performance of our method, the readings of the selected features are plotted against reference BYK wave-scan readings in Fig. 5 (provided by the manufacturer of ACT panels). The high correlation of our features to the reference is supported by Pearson’s correlation values and Spearman’s rank correlation index shown in Table 1. Rank ordering of ACT samples based on value of the proposed features in comparison with the reference ordering is shown in Fig. 6 and is demonstrating a good performance of the majority of the tested features.

Table 1: Relative values of standard deviations to mean values across the three readings of the same sample. Pearson’s correlations r_P and Spearman’s rank correlations index r_S between our features and ordering of a set of ten ACT panels

	SW	LW	AW	CA	CL	MA
RSD (%)	9.20	5.65	7.43	1.34	9.34	2.22
Corr. r_P	0.97	0.91	0.96	0.90	0.71	0.94
RCI r_S	0.96	0.95	0.99	0.93	0.77	0.96

Results for effect coatings

We analyzed one glass standard and ten effect coatings samples with the wave-scan device.⁶ In addition to the W_a - W_e wavelength ranges, it also provides readings of SW (short wavelength), LW (long wavelength), du (dullness), and DOI.

First, we calculated the Pearson correlation r between the results of our method and the readings of the wave-scan. The correlation of each wavelength range provided the following values: W_a : $r_P = 0.62$, W_b : $r_P = 0.84$, W_c : $r_P = 0.94$, W_d : $r_P = 0.91$ and W_e : $r_P = 0.58$. These results suggest high similarity of our method, especially for mid-range wavelengths. The lowest correlation is obtained for the bin W_e corresponding to the longest wavelengths. This is probably due to an insufficient representation of long wavelength in a highlight contour profile having a maximum length limited by circumference of a light source reflection. To improve representation of such wavelengths one would need to either increase the diameter of a light source or decrease its distance from the material.

Next, we evaluated the correlation of all our wavelength ranges and computational features with the wave-scan readings of SW, LW, dullness (du), and DOI, as shown in Table 2. Values in bold denote

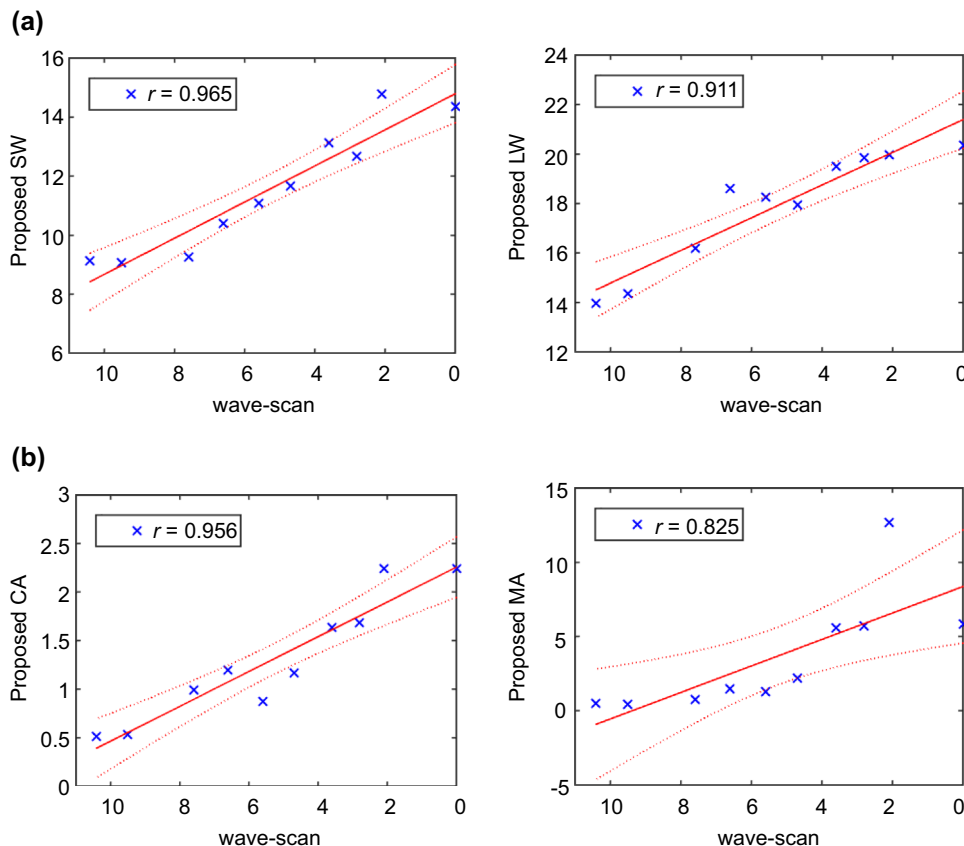


Fig. 5: Correlation plot between orange peel readings of ACT samples and (a) frequency features SW and LW, (b) computational features CA and MA

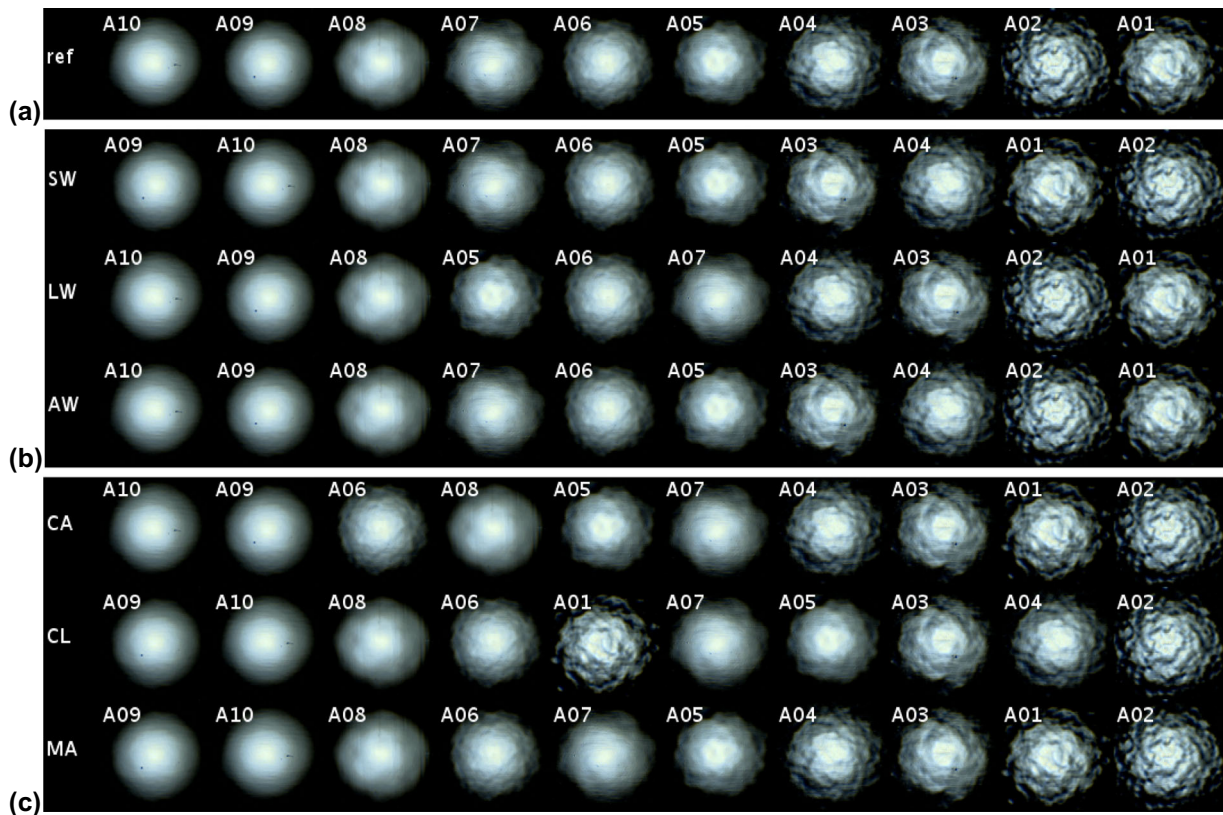


Fig. 6: ACT samples rank ordering based on: (a) wave-scan reference, (b) proposed frequency analysis features SW, LW, AW, (c) proposed computational features

Table 2: Pearson’s correlations r_P between computed frequency and statistical features (rows) with the wave-scan readings (columns). A more significant correlation values with p values lower than 0.05 are in boldface

Our features	BYK wave-scan features			
	SW	LW	du	DOI
W_a	0.89	0.45	0.39	- 0.44
W_b	0.89	0.57	0.41	- 0.45
W_c	0.79	0.78	0.25	- 0.28
W_d	0.77	0.80	- 0.04	- 0.01
W_e	0.90	0.51	- 0.06	- 0.13
SW	0.92	0.55	0.33	- 0.39
LW	0.85	0.78	0.10	- 0.15
AW	0.89	0.70	0.20	- 0.25
CA	0.76	0.61	- 0.15	0.08
CL	- 0.94	- 0.15	0.94	- 0.94
MA	0.58	- 0.08	0.59	- 0.62

statistically significant values having p value < 0.05 . We observe high correlations of all our frequency features to short wavelength SW of the wave-scan. Overall, the obtained higher correlation of the shorter wavelength bins to SW and the longer wavelength bins with LW is an intuitively correct behavior. The highest correlation to SW was obtained for the ranges W_a, W_b and the

highest correlation to LW was obtained for the ranges W_c and W_d . We also approximated LW by summing PSD contributions over wavelengths in the range of 1.2–12.0 mm and obtained $r_P = 0.78$ when compared to wave-scan LW. Our approximation of SW by summing PSD contributions over wavelengths 0.3–1.2 mm yielded a correlation of $r_P = 0.92$.

In contrast, high correlations to long wavelengths LW of the wave-scan are observed only for frequency features W_c, W_d and LW, which is intuitively expected behavior. A lower correlation value of W_e bin is related to physical size limitation of the reflected light source. Our computational features also mark a promising performance, namely relation of contour amplitude CA to the wave-scan SW and LW, contour length CL and mean average difference MA to the wave-scan SW, dullness, and DOI.

Figure 7 shows rank ordering of the test samples based on the value of the proposed features in comparison with the reference SW and LW orderings of the wave-scan device.

Results for challenging solid coatings

Finally, we performed additional analysis of three challenging solid coatings shown in Fig. 8. Sample P1 is

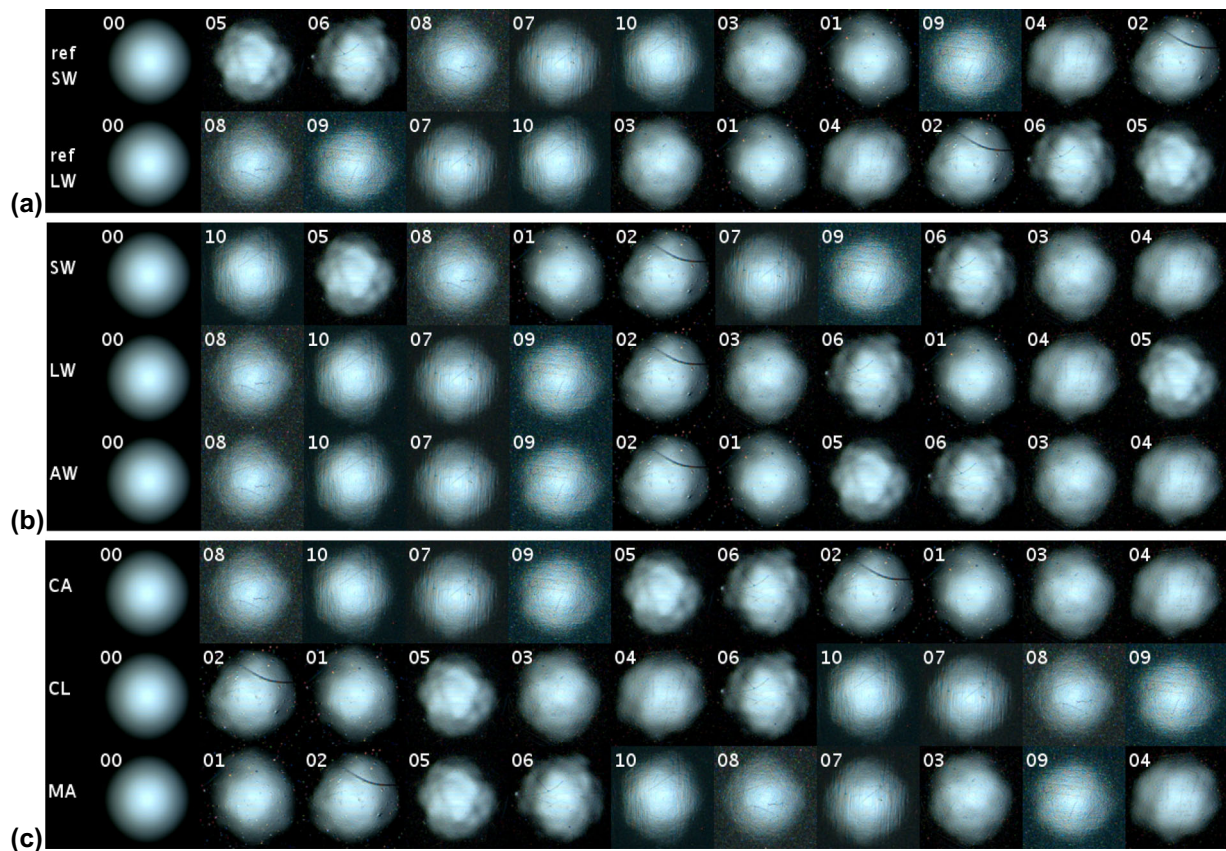


Fig. 7: Glass mirror and effect coating samples rank ordering based on: (a) reference wave-scan features SW and LW, (b) proposed frequency analysis features SW, LW, AW (c) proposed computational features

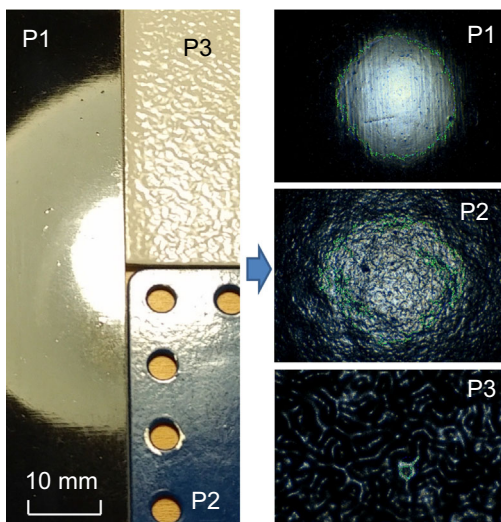


Fig. 8: Three solid coating material samples and their reflected contours

a plastic panel spray-coated by a glossy black paint. Samples P2 and P3 are powder-coated metal panels, where P3 exhibits extremely high decorative waviness. The figure also shows a light reflection from these

surfaces. Due to extreme waviness, our setup was not able to reliably detect highlight contour for sample P3 (see Fig. 8 right) and thus it was excluded from our analysis. Rank ordering of samples P1 and P2 within the ACT samples for features AW, CA, and MA is shown in Fig. 9. We observe that sample P1 has unidirectional grooves resulting from the plastic panel manufacturing process, affecting short to mid-wave wavelengths. P2 has a combined contribution of short and extremely low-range wavelengths, and therefore, it was always evaluated as an extreme waviness.

Discussion and limitations

The main advantage of the proposed method is that it is noncontact and does not place any requirements on the capturing system. In contrast to the setup presented in the literature,¹³ any standard camera and a light source with a reflection angle near 15° in a dark environment are sufficient.

Another advantage of the method is its low size requirement for the sample area. Although a bigger sample area is recommended, it is enough to capture an area comparable to the size of the reflected light source image.

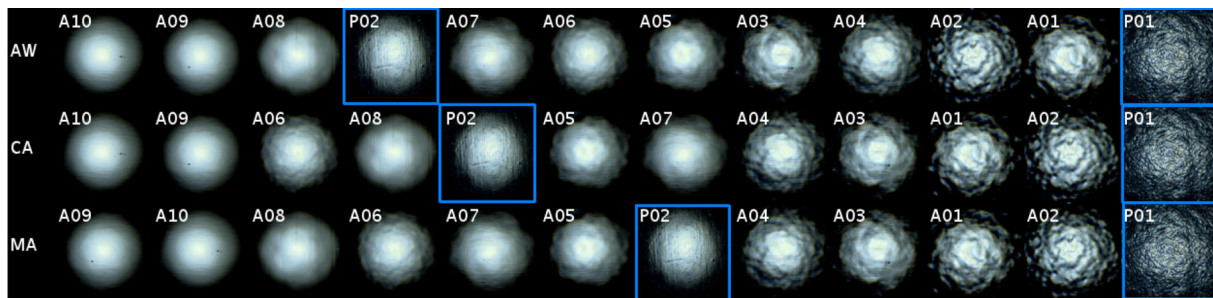


Fig. 9: Rank ordering of the solid coating samples from Fig. 8 within ACT orange peel standards for three selected features AW, CA, MA

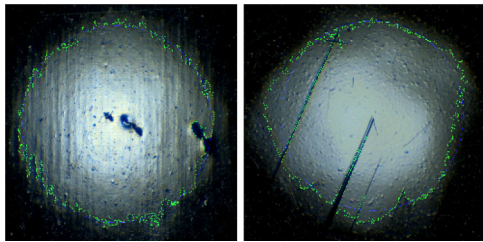


Fig. 10: Specular samples affected by a surface defect such as scratch, bubble, or dust

On the other hand, the main limitation of our method is that it captures sample information only from a small spot with respect to the size of the reflector; therefore, the method may be affected by local behavior that may not be typical for the material, such as scratches and dust, as shown in Fig. 10.

To limit impact of such defects, we recommend to scan multiple spots on the material sample and combine the results. In our experiments, we averaged readings of three spots, but capturing more spots is advisable for samples prone to surface defects.

If the size of the light source is too small, the very long wavelengths may be missing or underrepresented, resulting in a performance degradation. Our method works only on glossy surfaces that are able to reflect light source image. However, it can fail for glossy surfaces having high waviness, such that the reflected light cannot be detected as a continuous contour (see example of material P3 in Fig. 8).

The performance of our method depends on the physical size of the light source's reflected image and on the camera resolution. As the first factor can limit representation of low wave wavelengths, the second one may affect the method's sensitivity to small details. We compared results of our camera with resolution 2010 DPI, with results for camera having only 420 DPI, and obtained very similar performance with the main difference for short wave wavelengths W_a, W_b , suggesting that fine contour details were insufficiently represented at lower resolution. Therefore, it is recommended to have a minimum diameter of a light contour projection on the material over 1 cm, distance of light and camera from the sample around 30 cm, and camera resolution over 500 DPI.

Similarly to the previous work,¹³ we also tested an impact of weighting our PSD values using the contrast sensitivity function by Audi,¹⁷ but did not notice any significant change in performance of our features. We did not applied any scaling of the frequency bins $W_a \dots W_e$, but linear scaling of our values to BYK wave-scan reference readings provided the following scales: 0.50, 0.55, 0.95, 0.82, 0.85.

Conclusions

We proposed a noncontact method for orange peel analysis from a single image of a reflected circular light source. Our method is limited to glossy materials reflecting a continuous boundary of a circular light shape image. This boundary is obtained for a fixed intensity threshold applied to a high-dynamic range image captured at specular reflection geometry. A difference computed between this boundary and an ideal reflected ellipse provides information on normals' fluctuations along the boundary. We have shown that (1) analysis of the unfolded boundary profile in frequency domain and (2) features obtained from the boundary statistics have high correlation with readings of a commercial device. Our method was tested on a set of ten orange peel standards, ten effect coating samples, and additional three solid coating samples and can serve as a promising tool for affordable characterization of waviness on glossy surfaces.

Funding Open access publishing supported by the National Technical Library in Prague. This research has been supported by the Czech Science Foundation Grant GA22-17529S.

Conflict of interest The authors have no competing interests to declare that are relevant to the content of this article.

Open Access This article is licensed under a Creative Commons Attribution 4.0 International License, which permits use, sharing, adaptation, distribution and reproduction in any medium or format, as long as

you give appropriate credit to the original author(s) and the source, provide a link to the Creative Commons licence, and indicate if changes were made. The images or other third party material in this article are included in the article's Creative Commons licence, unless indicated otherwise in a credit line to the material. If material is not included in the article's Creative Commons licence and your intended use is not permitted by statutory regulation or exceeds the permitted use, you will need to obtain permission directly from the copyright holder. To view a copy of this licence, visit <http://creativecommons.org/licenses/by/4.0/>.

References

1. ASTM, D523-08, *Standard Test Method for Specular Gloss*. ASTM International, West Conshohocken, PA.
2. ASTM, D5767-95, *Instrumental Measurement of Distinctiveness-of-Image Gloss of Coating Surfaces*. ASTM International, West Conshohocken
3. ASTM, E430-19, *Measurement of Gloss of High-Gloss Surfaces by Abridged Goniophotometry*. ASTM International, West Conshohocken, PA.
4. Hunter, RS, et al., "Methods of Determining Gloss." NBS Research Paper RP 958
5. ASTM, E284-91, *Development of Standard Terminology of Appearance*. ASTM International, West Conshohocken, PA
6. wave-scan OrangePeel Meter, BYK-Gardner GmbH. <https://www.byk-instruments.com/en/appearance/wave-scan-orange-peel-meter/c/2344>, accessed 20/02/2023
7. Rhopoint TAMS - Total Appearance Measurement System, Konica-Minolta Sensing Europe b.v., <https://www5.konicaminolta.eu/ru/measuring-instruments/products/gloss-appearance-measurement/appearance-measurement/rhopoint-tams/accessories.html>, accessed 20/02/2023
8. Pfaff, G, Reynders, P, "Angle-dependent Optical Effects Deriving from Submicron Structures of Films and Pigments." *Chem. Rev.*, **99** (7) 1963–1982 (1999)
9. Maile, FJ, Pfaff, G, Reynders, P, "Effect Pigment - Past, Present and Future." *Prog. Org. Coat.*, **54** (3) 150–163 (2005)
10. Pfaff, G, *Special Effect Pigments: Technical Basics and Applications*. Vincentz Network GmbH & Co KG, Hannover (2008)
11. Brodmann, R, "Roughness Form and Waviness Measurement by Means of Light-scattering." *Precis. Eng.*, **8** (4) 221–226 (1986)
12. Konieczny, J, Meyer, G, "Computer Rendering and Visual Detection of Orange Peel." *J. Coat. Technol. Res.*, **9** (3) 297–307 (2012)
13. Sone, T, Watanabe, S, "Measurement and Evaluation Method of Orange Peel." *Electron. Imaging*, **2017** (8) 62–65 (2017)
14. Leloup, FB, Audenaert, J, Hanselaer, P, "Development of an Image-Based Gloss Measurement Instrument." *J. Coat. Technol. Res.*, **16** (4) 913–921 (2019)
15. ACT Orange Peel Standards, ACT Test Panels llc, <https://acttestpanels.com/products/> accessed 14/1/2023
16. Filip, J, Vávra, R, Maile, FJ, "Optical Analysis of Coatings Including Diffractive Pigments Using a High-Resolution Gonioreflectometer." *J. Coat. Technol. Res.*, **16** 555–572 (2019)
17. Kigle-Bockler, G, "Premiere for wave-scan 3 First Appearance." In: BYK-Gardner webinar, BYK-Gardner (2020)

Publisher's Note Springer Nature remains neutral with regard to jurisdictional claims in published maps and institutional affiliations.